frontiers | Frontiers in Earth Science

TYPE Original Research
PUBLISHED 20 March 2024
DOI 10.3389/feart.2024.1369742

OPEN ACCESS

EDITED BY
Aydın Büyüksaraç,
Çanakkale Onsekiz Mart University, Türkiye

REVIEWED BY
Funda Bilim,
Cumhuriyet University, Türkiye
Hanbing Ai,
China University of Geosciences Wuhan, China
Njeudjang Kasi,
University of Maroua, Cameroon

*CORRESPONDENCE
Fahriye Akar,
fahriyeakar@erzincan.edu.tr

RECEIVED 12 January 2024
ACCEPTED 12 February 2024
PUBLISHED 20 March 2024

CITATION
Akar F (2024), The upper crustal thermal structure of the Cameli Basin and its surroundings (SW Anatolia, Türkiye) by using the fractal-based centroid method of aeromagnetic data and its relationship with earthquakes occurring in the region. *Front. Earth Sci.* 12:1369742. doi: 10.3389/feart.2024.1369742

The upper crustal thermal structure of the Cameli Basin and its surroundings (SW Anatolia, Türkiye) by using the fractal-based centroid method of aeromagnetic data and its relationship with earthquakes occurring in the region

Fahriye Akar[1,2]*

[1]Earthquake Technologies Institute, Erzincan Binali Yıldırım University, Erzincan, Türkiye, [2]Construction Department, Vocational School, Erzincan Binali Yıldırım University, Erzincan, Türkiye

The Cameli Basin and its surroundings are located in southwestern Anatolia, Türkiye, and are one of the tectonically active regions in western Türkiye. The Curie point depth of continental crust can help us to determine the regional tectonic and geothermal structures. The aeromagnetic magnetic data of the study region were used to determine the Curie Point Depth estimates. The fractal-based centroid method is used for this purpose. The fractal approach removes the effect of fractal magnetization in the power spectrum. The depth to the bottom of the deepest magnetic sources in the study region ranges between 6.9 and 14.05. The estimated thermal gradient varies from 41.28°C/km to 89.23°C/km and the average value is 58.59°C/km (580°C for magnetite). The distributions of earthquakes are compatible with NW-SE trending estimated Curie depth anomalies. Interpretation indicates that the depth to the Curie isotherm is considerably shallower than the Moho depth.

KEYWORDS

South Western Türkiye, magnetic anomaly, Curie point depth, geothermal gradient, earthquake

1 Introduction

The magnetic method is very for understanding the thermal characteristics of a subsurface structure and geothermal information by analyses of magnetic data using the power spectral method. The Curie temperature, geothermal gradient, and heat flow can be associated with crustal thermal structure. The depth extent of crustal sources corresponds to the Curie temperature where magnetic rocks lose their spontaneous magnetization (e.g.; ~580°C for magnetite). The well-known method for determining the Curie Point Depth from magnetic data is the centroid method developed by Okubo et al. (1985). This method depends on analyzing the shape of the radial power spectrum calculated from the magnetic data in the Fourier domain (Spector and Grant, 1970;

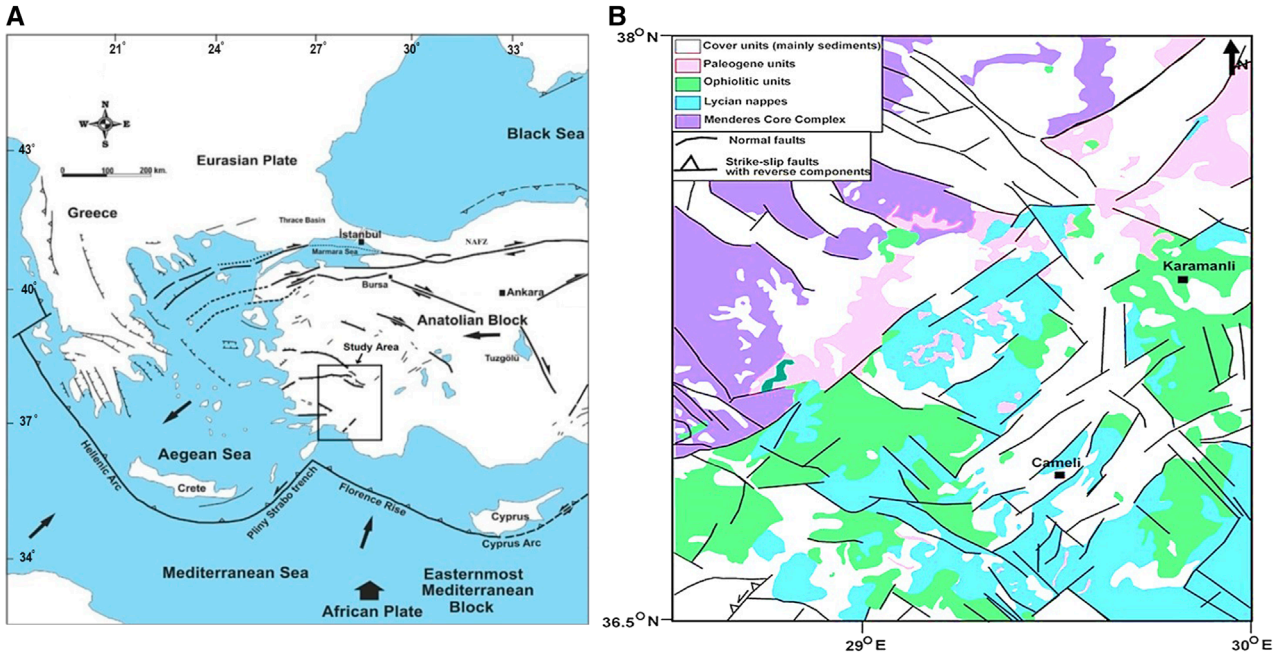

FIGURE 1
(A) Tectonic map of Türkiye (simplified from Över et al., 2023). **(B)** Geological map of the study area (simplified from Özkaptan et al., 2018).

Connard et al., 1983; Okubo et al., 1985).

The study area is situated in southwestern Türkiye (Figure 1A). Western Türkiye includes the most important geothermal region (e.g.; the Menderes Massif). Despite several tectonic and geologic research over the last four decades in western Türkiye (Sengor and Yilmaz, 1981; Bozkurt and Park, 1994; Hetzel et al., 1995; Bozkurt and Oberhansli, 2001; Bozkurt and Sozbilir, 2001; Gokten et al., 2001; Bozkurt, 2004; Seyitoglu et al., 2004; Alcicek et al., 2005; Alcicek et al., 2006; Westaway, 2006; Dilek and Altunkaynak, 2007; Oner and Dilek, 2013; Elitez et al., 2016; Roche et al., 2018; Schmid et al., 2020), there are a few geophysical studies based on the gravity/magnetic methods especially in the south of western and central Türkiye (Ates et al., 1997; Ates et al., 1999; Ates et al., 2005; Dolmaz et al., 2005; Dolmaz, 2007; Bilim et al., 2016; Aydemir et al., 2019; Erbek and Dolmaz, 2019; Pamukcu et al., 2019). Despite that, there are very limited geothermal studies based on the spectral analysis of magnetic data in southwestern Türkiye. Aydin et al. (2005) estimated the CPD of the whole of Türkiye from spectral analysis of aeromagnetic data without applied to any process (such as filter or/and the RTP process). They found that the CPD values were between 6 and 10 km in the Western Anatolia. Dolmaz et al. (2005) determined the CPD for Western Anatolia ranging between 8.2 and 19.9 km by using the spectral analysis of the RTP anomalies of aeromagnetic data and selected the fixed window range as 90 km. Bilim et al. (2016) determined the CPD values of the Aegean region and the Menderes Massif by using the centroid method (Okubo et al., 1985) (the constant window range as 70 km). They suggested that the CPD values are shallower than the Moho depth in the Menderes Massif and the Aegean region. Recently, Erbek and Dolmaz, (2019) estimated the CPD and heat flow values of the aeromagnetic data of the southeastern Aegean Sea using the centroid method (Okubo et al., 1985) (the constant window range as 90 km). They calculated as 100–120 mWm^{-2} for Denizli city and its surrounding area.

In this article, the crustal structures of the Cameli Basin and its surroundings are determined by the Curie point depth (CPD) (i.e.; the base of the magnetized layer within the crust) for the first time using the fractal-based centroid method (Fedi et al., 1997; Li et al., 2009) applied to the RTP magnetic anomalies. An article on a similar topic in the same geographical region was recently published by Akar and Bilim, (2022). Different methods (such as RTP and analytical signal) were used in the study of determining the crustal structure under the Cameli Basin (SW Türkiye) using aeromagnetic data. The area they examine is narrower. In this article, geothermal research was conducted in a wider area using the fractal-based centroid method.

Anatolia is under the influence of tectonic elements such as the right-lateral strike-slip North Anatolian Fault Zone (NAFZ), the left-lateral slip-slip Eastern Anatolian Fault Zone (EAFZ), and the Aegean graben system. The Anatolian plate is moving westwards along the NAFZ from the north, due to the north-northwest movement of the African plate from the south and the opening regime of the Red Sea, and the Arabian plate moving towards the north. However, the African plate is diving under the Anatolian plate in the Mediterranean. Thus is formed the Hellenic-Cyprus arc (Sengor et al., 1984).

Southwestern Türkiye is characterized by a complex neotectonic deformation that results from the West Anatolian externational processes associated with Anatolian extrusion and those related to the eastern Hellenic roll-back (Sengor and Yilmaz, 1981). Subduction zone roll-back has resulted in a series of sinistral strike-slip zones that penetrate into SW Türkiye, where the fault zones

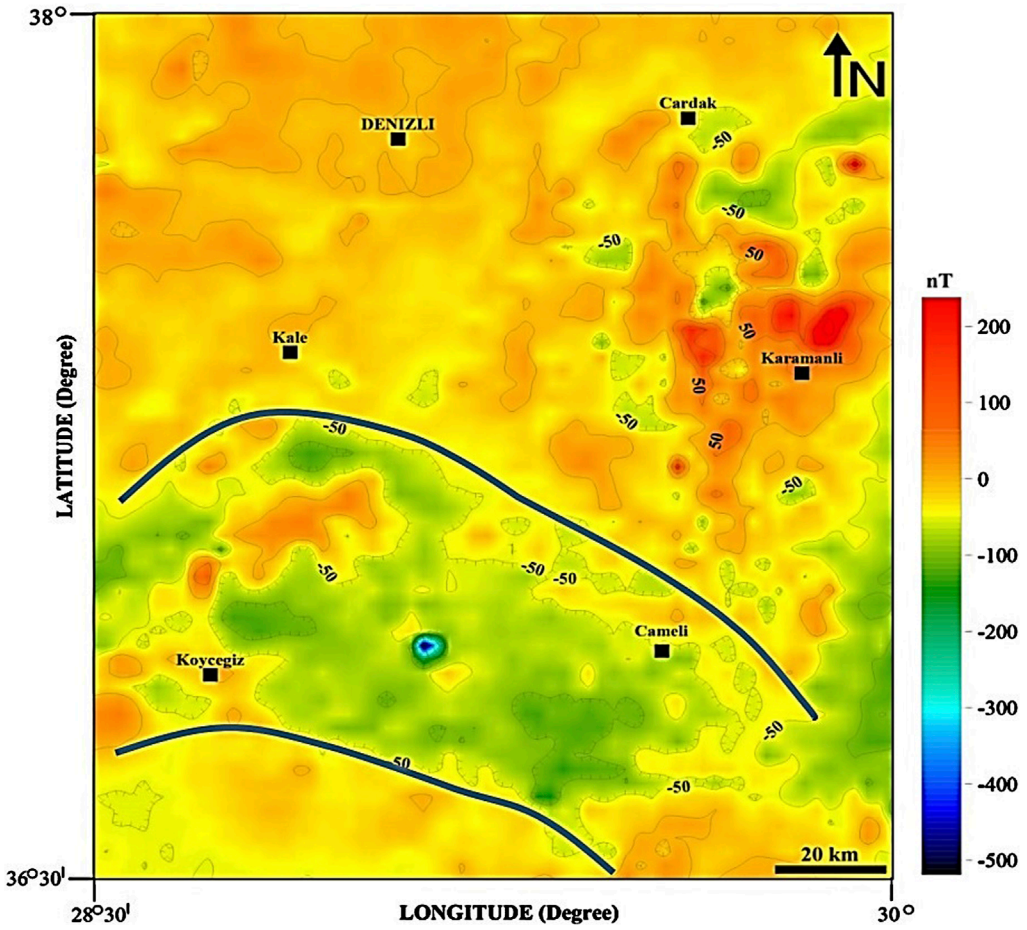

FIGURE 2
Residual aeromagnetic anomaly map of the study area.

are represented by many sub-parallel fault segments called Fethiye-Burdur Fault Zone (FBFZ) (Teen Veen et al., 2009).

The FBFZ is a transtensional left-lateral shear zone 75–90 km wide and 300 km long (Elitez et al., 2016). Elitez et al. (2016) determined that the middle section of the zone consists of an ancient basin fill including the middle Miocene to lower Pliocene sequence, accumulated in fluvial and lacustrine environments and deformed by left-lateral transtensional shearing. On the other hand, some researchers mention that the FBFZ is the on-land continuation of Pliny-Strabo fault system that is thought to be a strike-slip zone (Over et al., 2010; Over et al., 2010) suggested that the FBFZ is characterized by late Miocene-Quaternary NE-SW trending faults and basins (e.g.,; Cameli, Burdur, and Acigol Basins). Cameli Basin is located on the NE-SW oriented BFFZ, in this region where tectonic activity is quite intense in southwestern Anatolia (Yaltırak et al., 2010).

The tectonic development, tectonostratigraphic evolution, and geology of the Cameli Basin have been studied in detail by some researchers (Alcicek et al., 2005; Alcicek et al., 2006; Teen Veen et al., 2009). Alcicek et al. (2006) proposed that in the Cameli Basin, the youngest deformation is characterized by dextral shear along NE-SW-trending strike-slipe faults in combination with continuing NW-SE extension. Alcicek et al. (2005) said that the Cameli Basin was fully terrestrial and hosted lacustrine, fluvial, and alluvial-fan depositional systems including river deltas and fan deltas of both shoal-water and Gilbert type.

The surface of the study area is mostly covered by younger sediments (Figure 1B). The Lycian Nappes and ophiolitic units are outcrops found around the center and south of the study area. The basement unit of the Cameli Basin consists of the Lycian allochthon units (Alcicek et al., 2005). The Lycian Nappes consist of Palaeozoic rocks, Mesozoic volcanic rocks, Mesozoic sedimentary rocks, Mesozoic limestone, Cretaceous ophiolitic melange, Cretaceous flysch, and Palaeogene sedimentary rocks (Elitez et al., 2016).

The rocks of Menderes Massif are exposed on the north-western side of the study area (Figure 1B). The south of Menderes Massif located on the eastern margin of the Aegean region is bordered by the Lycian nappes (Alcicek et al., 2005).

2 Materials and methods

The fractal approach removes the effect of fractal magnetization from the observed power spectrum and estimates the upper depth and lower depth parameters of the magnetized layer

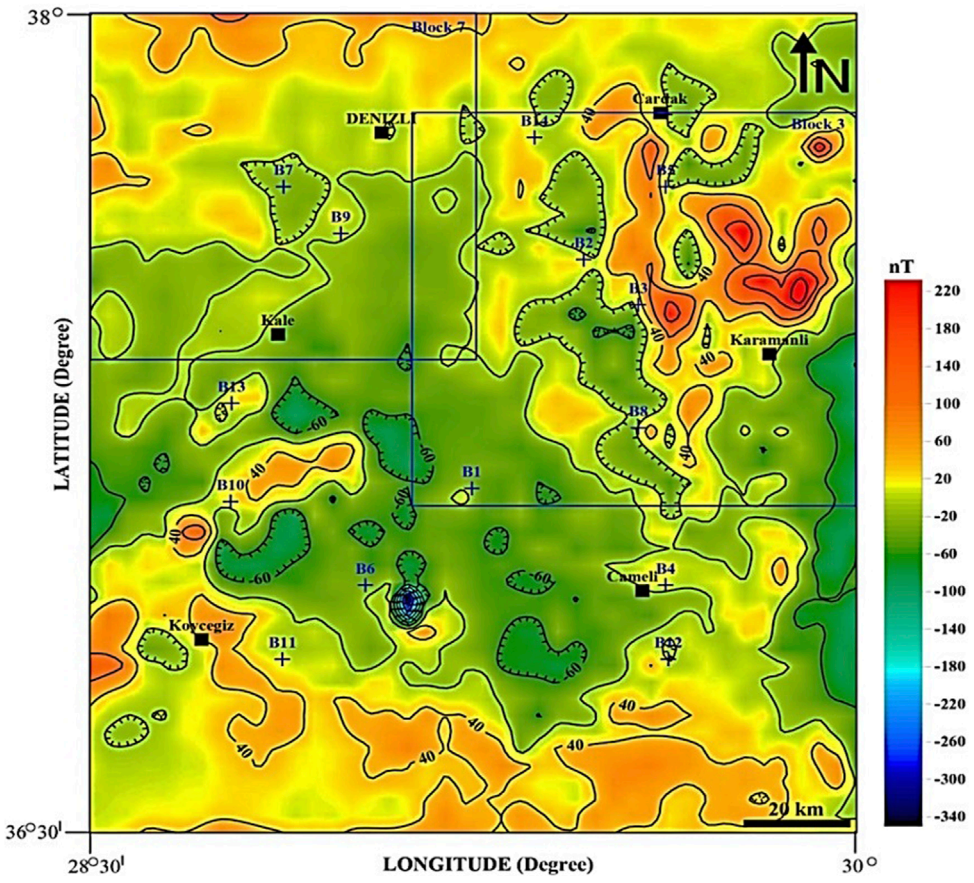

FIGURE 3
The RTP anomalies were applied to the residual aeromagnetic anomaly data.

using iterative forward modeling of the power spectrum (Pilkington and Todoeschuck, 1993a). The advantages of this method are that the range of applicable fractal parameters can be estimated and the depth of magnetic field sources or anomalies to the base can be obtained based on simultaneous estimation of depth values from the center of gravity method and visual inspection of the forward modeling of the spectral peak (Khojamli et al., 2017). The ability to determine the fractal parameter range is considered an advantage of the fractal method. Additionally, this method can be used to simultaneously estimate the depth to the base of magnetic sources through forward modeling of the centroid method and the spectral peak method (Shirani et al., 2020).

The Curie-temperature isotherm corresponds to the basal surface of the magnetic crust and can be calculated from the lowest wavenumbers of magnetic anomalies (Ross et al., 2006; Nabi, 2012; Bilim et al., 2016). The centroid method developed by (1) is one of the most popular methods to infer the depth of CPD. The centroid method is generally based on the (Spector and Grant, 1970) method that uses the power spectra of magnetic anomalies created by ensembles of rectangular vertical magnetic prisms related to geological structures. The slopes of logarithms of Fourier spectra of magnetic data are related to the depth to the top of the magnetic sources.

The azimuthally averaged power spectrum is

$$\varphi(|k|) = Ae^{-2|k|z_t}\left(1 - e^{-2|k|(z_b - z_t)}\right)^2 \quad (1)$$

Where A is a constant; k is the wavenumber; and zt and zb are the top and bottom depths of the magnetic source, respectively (Bhattacharyya and Leu, 1975; Okubo et al., 1985). $\varphi(|k|)$ is the radially averaged power spectra of the magnetic anomalies. By taking the logarithm of both sides of Eq. 1, it is obtained

$$\ln \varphi(|k|) = \ln A - 2|k|z_t + 2\ln\left(1 - e^{-|k|(z_b - z_t)}\right) \quad (2)$$

For wavelengths less than about twice the thickness of the layer, Eq. 2 can be written as

$$\ln\left(\varphi(|k|)^{1/2}\right) = \ln B - |k|z_t \quad (3)$$

The slope of the medium-high wavenumber portion of the power spectra shows the top of the magnetic source (z_t). By setting $z_0 = (z_t + z_b)/2$, which is the centroid depth of the magnetic source, Eq. 1 can be rewritten as

$$\varphi(|k|)^{1/2} = Ce^{-|k|z_0}\left(e^{-|k|(z_t - z_0)} - e^{-|k|(z_b - z_0)}\right) \quad (4)$$

At long wavelengths, Eq. 4 can be written as follows

$$\varphi(|k|)^{1/2} = Ce^{-|k|z_0}\left(e^{-|k|(-d)} - e^{-|k|d}\right) \approx Ce^{-|k|z_0}.(2|k|d),$$
$$\ln\left(\varphi(|k|)^{1/2}/|k|\right) = \ln D - |k|z_0 \quad (5)$$

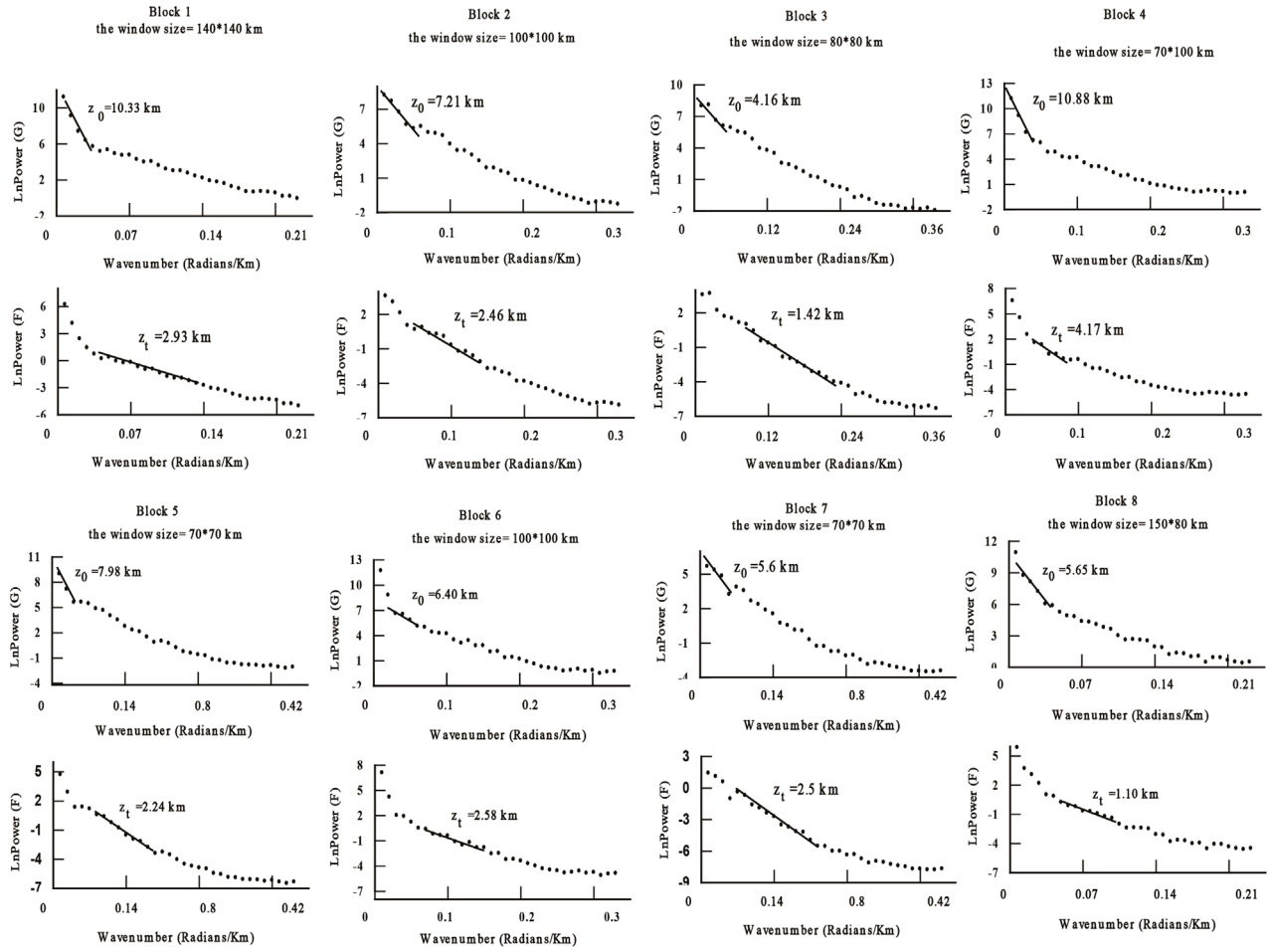

FIGURE 4
Spectral analysis results of Blocks 1–8. The depths (z0 and zt) are estimated from the fractal-based centroid method from the RTP data.

where C and D are constant $2d$ is the thickness of the magnetic layer and z_0 is the centroid depth of the magnetic source (Okubo et al., 1985).

The power spectra may include a fractional noise (Berry et al., 1980; Turcotte and Schubert, 1982; Fedi et al., 1997) that causes an overestimation of the depth value. Therefore, the power spectra are proportional to the frequency raised to a scaling exponent ($-\beta$), which is related to the fractal dimension (Fedi et al., 1997; Li et al., 2009). The corrected Eq. 3 and 5 can be rewritten as

$$\ln\left(|k|^{(\beta-1)/2}\varphi(|k|)\right) \approx \ln B - |k|z_t \tag{6}$$

and

$$\ln\left(|k|^{(\beta-1)/2}\varphi(|k|)/|k|\right) \approx \ln D - |k|z_0 \tag{7}$$

Where β is the fractal scaling parameter of magnetization. The Curie point depth (z_b) is estimated from

$$z_b = 2z_0 - z_t \tag{8}$$

Thermal gradient values can be estimated using a simple equation, $gradT$=580°C/z_b (Okubo et al., 1985). The Curie temperature of pure magnetite is assumed as 580°C for the calculation of the above-mentioned gradients.

2.1 Magnetic data

The aeromagnetic data of the study region were obtained from the General Directory of Mineral Exploration and Research (MTA) of Türkiye (CUBAP Project: M567). The flight line of the aircraft is 600 m from the ground surface. International Geomagnetic Reference Field (IGRF) was removed from the original data using a computer program supplied by Baldwin and Langel, (1993). The image map of the resulting aeromagnetic anomalies after the removal of the IGRF is shown in Figure 2. Reduction to the pole transformed (RTP) (Blakely Richard, 1996) was applied to the residual aeromagnetic anomalies of the study region (Figure 3). Distortions occur due to the Earth's magnetic field and magnetization. This makes the interpretation of aeromagnetic anomalies difficult. The RTP method is used to eliminate magnetic anomaly distortions (Ates et al., 2012).

Generally, anomalies are in harmony with surface geology. Young sedimentary units of the Cameli Basin show negative magnetic anomalies (−150 nT). The high elliptical-shaped magnetic anomalies in the northwest of the Cameli Basin are mainly related to the basement rocks that are composed of Lycian nappes outcropped from the faults bounding the Cameli Basin. High

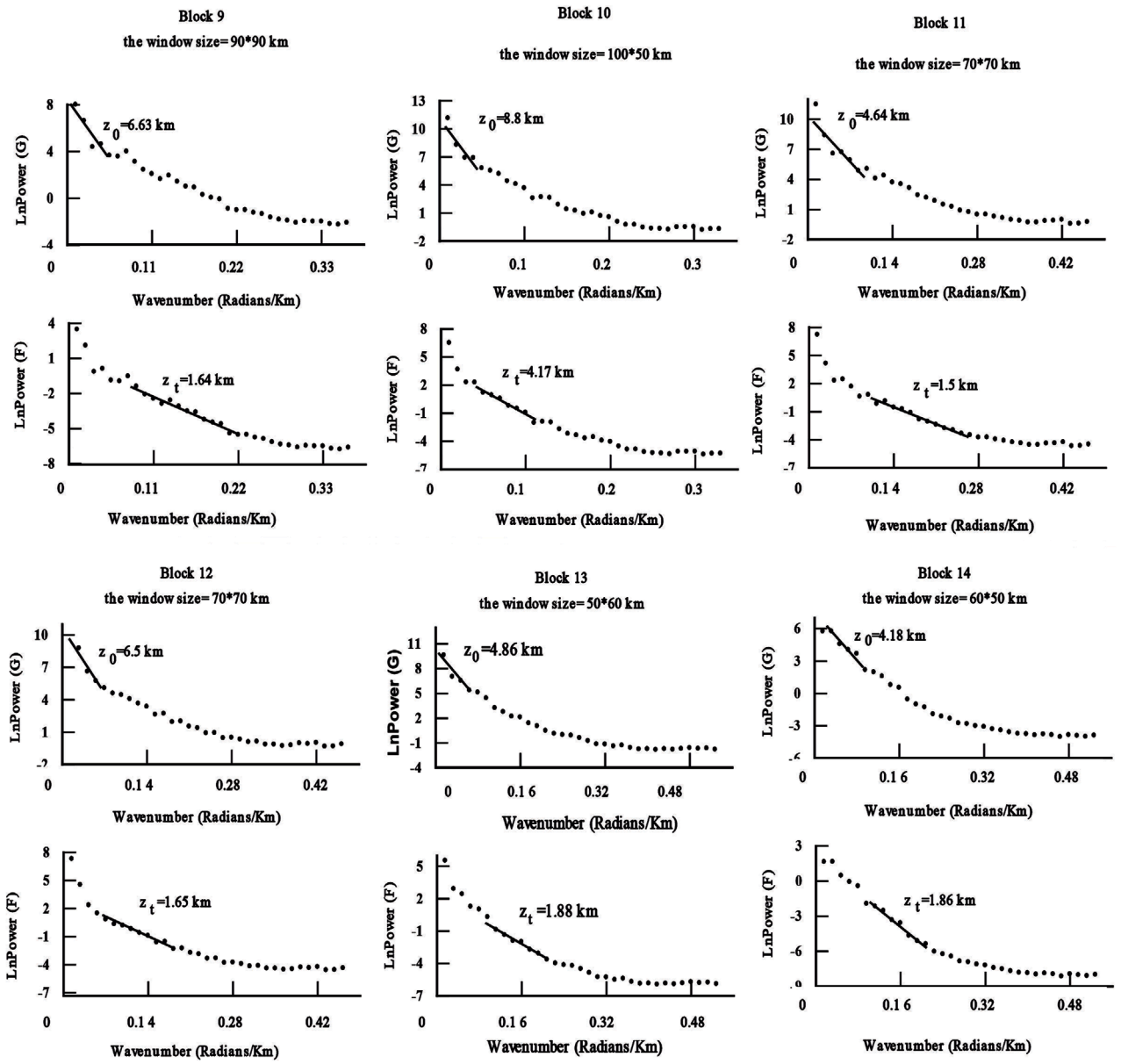

FIGURE 5
Spectral analysis results of Blocks 9–14. The depths (z_0 and z_t) are estimated from the fractal-based centroid method from the RTP data.

magnetic anomalies are represented by volcanic rocks and fault zones. The volcanic outflow in Figure 3 is thought to be associated with earthquakes.

3 Results and discussion

The Curie-point depths (also known as magnetic bottom) values and geothermal gradient play an important role in the determination of the thermal characteristics of a region. These physical values are important for locating areas that contain a high geothermal potential. In this study, the CPD of the Cameli Basin was estimated using the de-fractal spectral analysis method from magnetic data. For this purpose, the RTP process is firstly applied to total magnetic data (Figure 2) in the Fourier domain that retrieves data as they would be observed at the geomagnetic north pole, simplifying their shape and repositioning them above the causative bodies (Figure 3). The RTP converts the symmetry of the anomaly into a symmetric shape. The declination and inclination angles of Earth's magnetic field were taken as 4°E and 55°N, respectively in the RTP processes. Second, the magnetic anomaly map reduced to the RTP (Figure 3) was divided into 14 overlapping blocks having the moving windows selected with different window sizes between 50 km and 150 km. According to Blakely Richard, (1996) the block size of the grid for spectral analysis should be at least 5–6 times the expected magnetic depth. The minimum Curie depth was determined as about 8–10 km for western Anatolia (Dolmaz et al., 2005). Therefore, in this study, the lower and upper limits of window sizes were taken as 50 km and

TABLE 1 Curie point depths (CPD) and thermal gradient (grad *T*) values for each block in the study area.

Block Number	Depth to Centroid (z_0) km	Depth to Top (z_t) km	Curie point Depth (z_b)km	Geothermal Gradient (°C/km)
Block 1	10.33	2.93	14.05 ± 0.93	41.28
Block 2	7.21	2.46	11.96 ± 0.36	48.50
Block 3	4.16	1.42	6.90 ± 0.98	84.05
Block 4	10.88	4.17	13.71 ± 0.83	42.30
Block 5	7.98	2.24	13.72 ± 0.84	42.27
Block 6	6.40	2.58	10.22 ± 0.09	56.75
Block 7	5.60	2.50	8.70 ± 0.49	66.66
Block 8	5.65	1.10	10.20 ± 0.09	56.86
Block 9	6.63	1.64	11.62 ± 0.28	49.91
Block 10	8.80	4.17	13.43 ± 0.76	43.18
Block 11	4.64	1.50	7.78 ± 0.74	74.55
Block 12	6.50	1.65	1.35 ± 0.20	51.10
Block 13	4.86	1.88	7.84 ± 0.72	73.97
Block 14	4.18	1.86	6.50 ± 1.08	89.23

150 km, respectively. Third, the radially averaged power spectrum in the Fourier domain is calculated for each block using Equations (6) and (7) after the fractal corrections (β). The top (z_t) and centroid depths (z_0) of the magnetic sources are estimated from Eqs (6) and (7), respectively. Pilkington and Todoeschuck, (1993b) proposed a constant fractal exponent (β) of 2.08–2.72 for igneous rocks. Fedi et al. (1997) applied the centroid method assuming a constant fractal exponent as 3. We also selected the fractal scaling parameter as β =3 in Eqs (6) and (7). The radially averaged power spectrum graphs of the power spectral density against wavenumbers were produced for each block. To obtain the depths to the top and centroid of the magnetic layer, the least-square method was used by fitting certain parts of the power spectrum graph with high and low wavenumbers. At very long wavelengths, the hyperbolic sinc tends to unite, leaving a single term of the centroid, z_0 (Okubo et al., 1985). The depths to the top, z_t, were estimated through the slope of the high-wavenumber part of the logarithm of the spectrum (Figures 4, 5). Finally, the CPD values (z_b) of all blocks were estimated by the centroid method with fractal magnetization using $z_b = 2z_0$-z_t (Eq. (8)) for the first time in this study (Table 1).

Figure 6 shows the Curie depth distribution in the study area. The Curie point depths of the study area range between about 7 and 14 km (Table 1). The deeper depth values are located at the Cameli Basin and vary from 11 to 14 km. The deepest Curie anomalies display the NW-SE trending elliptical contour closure, where covered with mainly the basin's youngest deposits. The deposits were generated by the FBFZ bounding the NE-SW Cameli Basin (Elitez and Yaltirak, 2016). The deepest Curie values correlate well with large sedimentary units in the study area. It can be suggested from estimated z_t values that the sediment thickness varies between 1.14 km and 4.17 km (Table 1).

In addition, it is assumed that the magnetic layer is below the sedimentary layer in the Cameli Basin. The distribution of the earthquakes is densely accumulated in the two regions: 1) the west of Cameli district, and 2) the north of the study area, around Denizli town (Figure 6, filled with black circles). The distributions of earthquakes are more compatible with NW-SE trending estimated Curie depth anomalies (Figure 6). Additionally, Figure 7A) shows the CPD and all earthquake focal depths in the west-east direction A-A′ section drawn in Figure 6. Figure 7B), shows the CPD and all earthquake focal depths in the South-North direction B-B′ section drawn in Figure 6. The crustal thickness (Moho depth) varies between 25 and 34 km in western Türkiye (Saunders et al., 1998) and according to Ates et al. (2012), the crustal thickness of our study area varies between 30 km and 35 km. The calculated Curie depths lie above the Moho in the study region. It is proposed that magnetic bodies caused by magnetic anomalies could have emplaced in the upper crust during the NW-SE extension of Cameli Basin. Akar and Bilim, (2022) determined two distinct states of stress characterized by nearly orthogonal NW-SE and NE-SW σ_3 axis in the Cameli Basin by using the fault kinematic analysis and inversion of the focal mechanism of shallow earthquakes. They also proposed that the NW-SE extension is attributed to the subduction process along the Cyrus arc. The Anatolian Plate and the Arabian Front thin from north (~44 km) to south (~36 km), which means a shallow Curie point depth (12–16 km) (Elitok and Dolmaz,

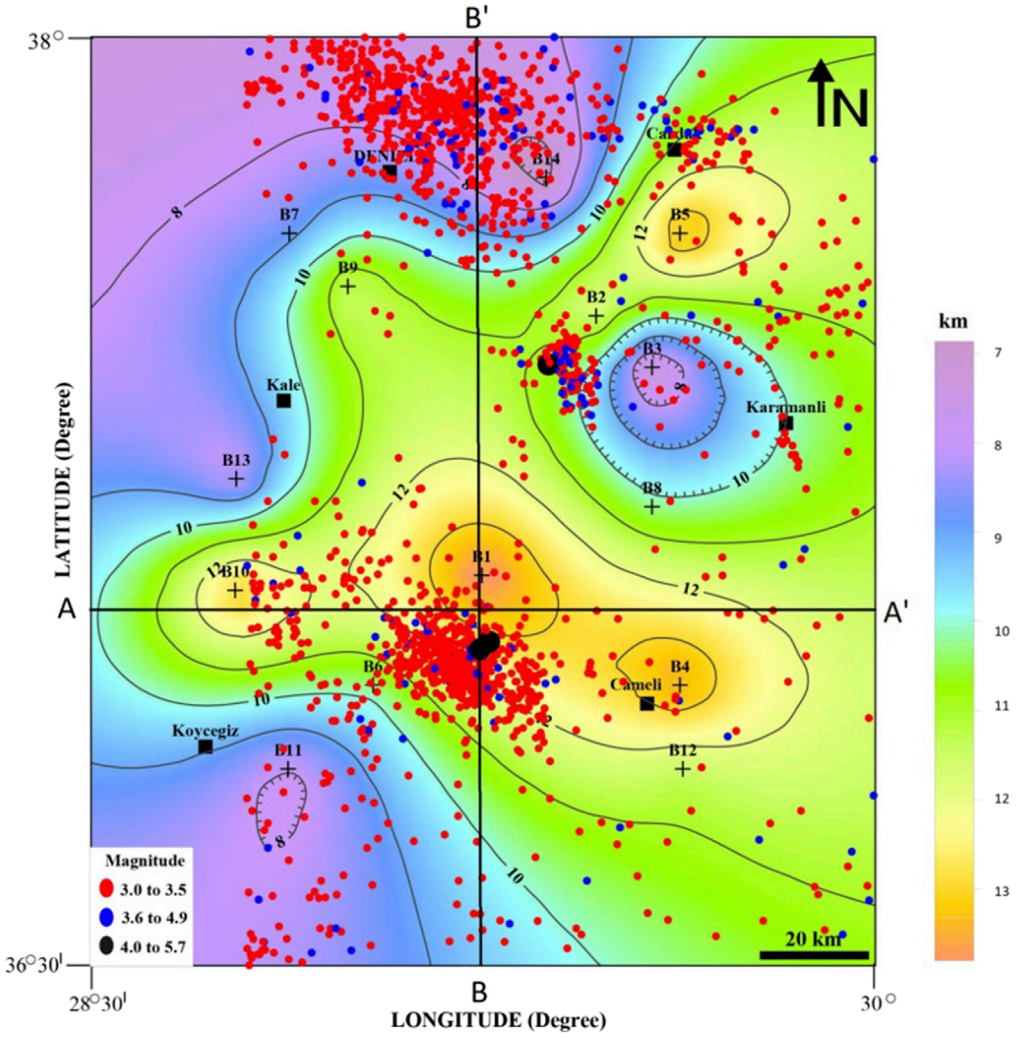

FIGURE 6
Estimated Curie Point Depth (CPD) map from the residual aeromagnetic anomalies of the study area. Contour interval: 1 km. (+) sign shows the centers of the blocks. Circles show epicenters of earthquakes with M ≥ 3.0 between 2010 and 2022 occurred in the study region.

2008). Pamukçu et al. (2014) found that shallow Curie point depths (~12 km), high heat flow values (~80 mW/m 2), and thin crust in the north and northwest of the Bitlis-Zagros Suture Zone are associated with volcanic and geothermal areas. Researchers such as (Li et al., 2019; Abdullahi and Kumar, 2020; Ma et al., 2023; Yaro et al., 2023) also used this fractal method in determining the Curie depth to reveal the thermal structure.

Three significant shallow thermal anomalies (7–8 km Curie depth) are determined from the fractal-Curie depth map (Figure 6). One of the areas is located around Denizli town on the northern border of the study area. This area is located at the Menderes Massif. Dolmaz et al. (2005) found Curie depths of 12 km. Our estimated CPD values and map are different from the results of (22) in the Denizli area. One reason for the difference is that (22) applied the method of (1) for large regional areas without using the scaling properties of the source distributions. However, our results are well correlated with the study of (Bilim, 2007) determined the shallow contour closure in the CPD map (<9 km) for the Denizli area despite not using the fractal method. The Denizli area is the highest geothermal system in western Anatolia (the well reservoir temperature = >200°C, Haklidir and Haklidir, (2020).

Our results are also well correlated with the study of Ilkisik, (1995). He determined the heat flow of 170–193 mWm^{-2} from silica temperature measures of thermal springs in the north of Denizli. However, these thermal springs could not be shown on the map as they coincide with the northern border of the study area (Dolmaz et al., 2005) produced by the heat-flow contour map of western Anatolia from magnetic data. Their heat flow values for the Cameli basin and its surroundings range from 60 mWm^{-2} to 100 mWm^{-2}. Heat flow contours decrease from northwest to southeast and are inversely related to estimated curie values (Figure 6). The heat flow values can correlate with tectonism in continents. Continental extension and tectonically active regions such as western Anatolia display high heat flow values.

The shallow Curie depths area also shows higher heat flow values. The other two shallowest curie anomalies determined in this study are located southeast of Koycegiz (the lower left corner of the study area) and west of Karamanli (Figure 6). Both areas exhibit

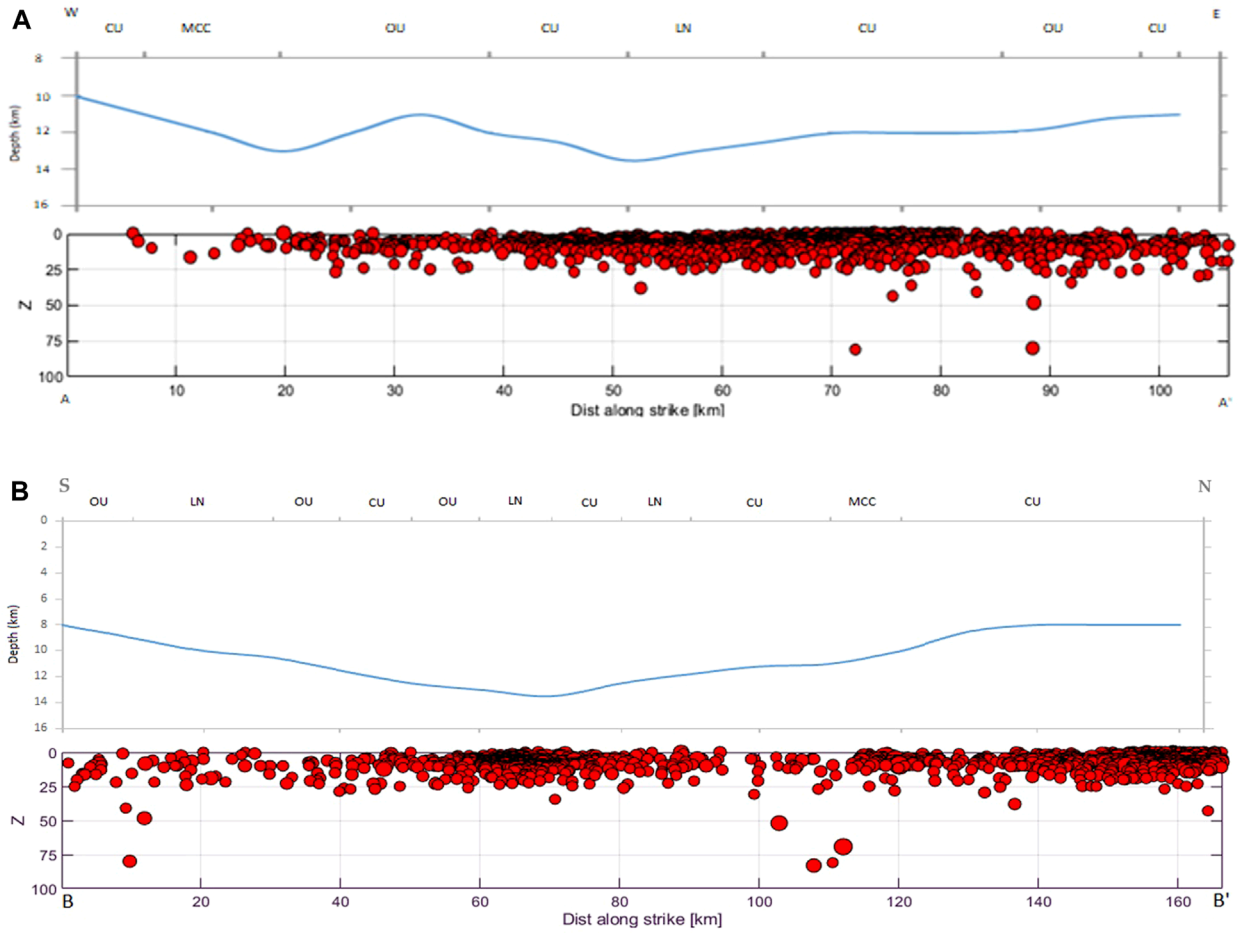

FIGURE 7
(A) The CPD and all earthquake focal depths in the west-east direction A-A′ section drawn in Figure 6. **(B)** The CPD and all earthquake focal depths in the South-North direction B-B′ section are drawn on it. Here, CU: Cover units, PU: Paleogeneunits, OU: Ophiolitic Units, LN: Lycian nappes, MCC: Menderes core complex represent.

approximately circular contour closures and can be associated with mainly ophiolitic units of Lycian nappes. These two shallow Curie anomalies could not be seen in the Curie depth map (Dolmaz et al., 2005). The study area of (29) did not include the Cameli Basin and its south.

The thermal structure also constitutes a high thermal gradient and many researchers used 580°C for determining the geothermal gradient values from the CPD. The geothermal gradient map of the study region (Table 1; Figure 8) was produced from grad T= 580°C/z_b (Okubo et al., 1985).

The obtained results also show the geothermal gradient is between 41°C and 89.23°C km^{-1} in the study area (Table 1; Figure 8). These values are higher than a typical geothermal gradient of ~25°C km^{-1} in continental crust (Lowell and Rona, 2005).

According to (Büyüksaraç, 2005), magnetic anomalies are generally seen in two different shapes: elliptical and circular. Of these, circular anomalies indicate volcanic outflows, while elliptical anomalies indicate structural changes. High and positive magnetic anomalies in Figures 2, 3 indicate areas with high magnetization. In this study, high magnetic anomalies are thought to be associated with volcanic rocks, and fault zones and represent the Lycian Nappes and especially mountainous areas.

The influence of the Helen-Cyprus arc in the region where the earthquakes occurred [the distribution of earthquakes is in the form of an arc (Figure 9)] and the coherence of the magnetic anomalies is clearly observed. The effects of various discontinuities in the study area are also seen as elliptical magnetic masses in Figure 3.

Figure 9B, which includes earthquakes larger than 2 that occurred between 2004 and 2020 in the south of the study area, and Figure 7A,B show deep-focus earthquakes. An interesting phenomenon that first attracted the attention of researchers such as (Akar et al., 2022) is the presence of deep-focus earthquakes with a depth of more than 60 km in this region. Accordingly, some earthquake focus was thought to be located in the Upper Mantle. This indicates that there is a difference between the tectonic character of this region and other regions (Ergin, 1966). It is also noteworthy that the earthquake intensity is at shallow Curie point depths.

Over et al. (2010) suggested that the influence of the Hellenic arc is dominant in the west of southwestern Türkiye and the influence of the Cyprus arc is dominant in the east of southwestern Türkiye.

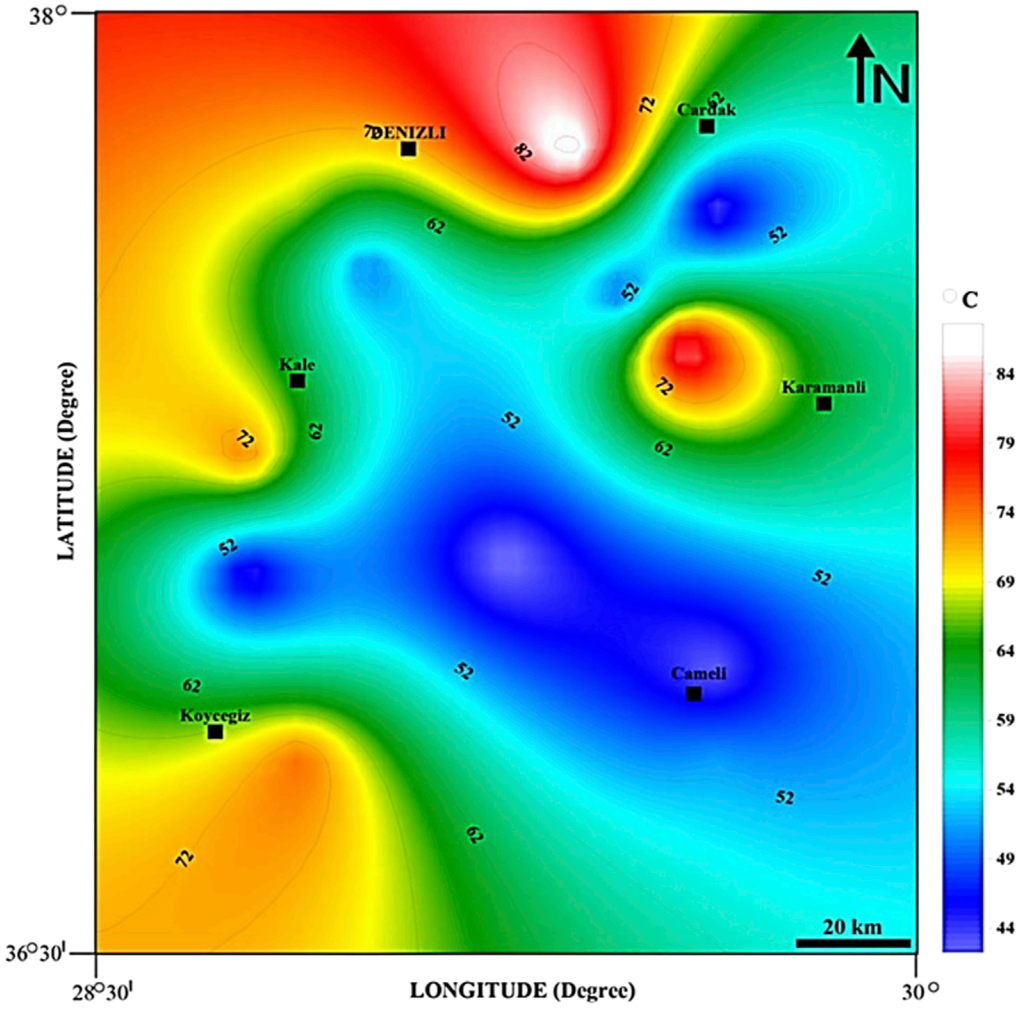

FIGURE 8
Geothermal gradient (580°C/km) map of the study area calculated from the Curie Point Depths (CPD). Contour interval: 5°C/km.

They stated that the Cameli Basin was stretched NW-SSE in the Late Miocene under the influence of the Cyprus Arc and then shifted to an NE-SW stress system under the influence of the Hellenic Arc.

The counterclockwise (N-SSE) motion of the Anatolian-Aegean region ranges from 20 mm/yr in central Anatolia to 30 mm/yr near the Hellenic trench (Reilinger et al., 2010). The western extension zone of the Anatolian plate is deformed by the opening of the arc behind the Hellenic and Cyprus arcs (Bozkurt, 2001).

The Helen-Cyprus arc is defined as a left-lateral strike-slip fault with a reverse fault component extending from the south of Crete and the island of Rhodes to the south of Türkiye towards the Gulf of Fethiye (Demirtaş, 2018).

Figure 9 shows that the Helen arc is clearly visible both in the surface distribution of earthquakes (between the blue lines) and in the depth distribution. In other words, due to this subduction zone causing the Helen arc, earthquakes can occur at depths of more than 60 km in the region. Therefore, deep focussed earthquakes are also observed in this region.

There are many faults that produce earthquakes in the study area. There is the Cameli basin, which was formed under the influence of the north-south direction extensional regime. There are normal faults such as the Dirmil Fault in the southeast of this basin and the Bozdağ Fault in the northwest (Alcicek et al., 2005; Alcicek et al., 2006).

Some of the most active and important faults in the region are located in the fault zone extending in the NE-SW direction between Burdur and the Mediterranean. The NE-SW trending Fethiye-Burdur Fault Zone, located in the northeast of the Cameli basin, constitutes the main fault zone in the region. Babadağ Fault, Honaz Fault, Kaleköy Fault, Karakova Fault and Pamukkale Fault extending between Honaz-Pamukkale-Karahayıt, fault extending between Honaz-Kaleköy and Özerlik-Sarayköy passing in the near NE of the Denizli basin; the faults extending between Honaz and Karakova constitute other important faults in the study area (Çubuk, 2010).

Earthquakes occur in wide zones where continents collide and indicate that the deformations there are complex (Alptekin, 1973). Earthquakes in Southwest Anatolia are related to the westward movement of the Aegean-Anatolian block as well as the subduction zone (Dewey and Sengör, 1979) as in the section shown as a blue arc in Figure 9.

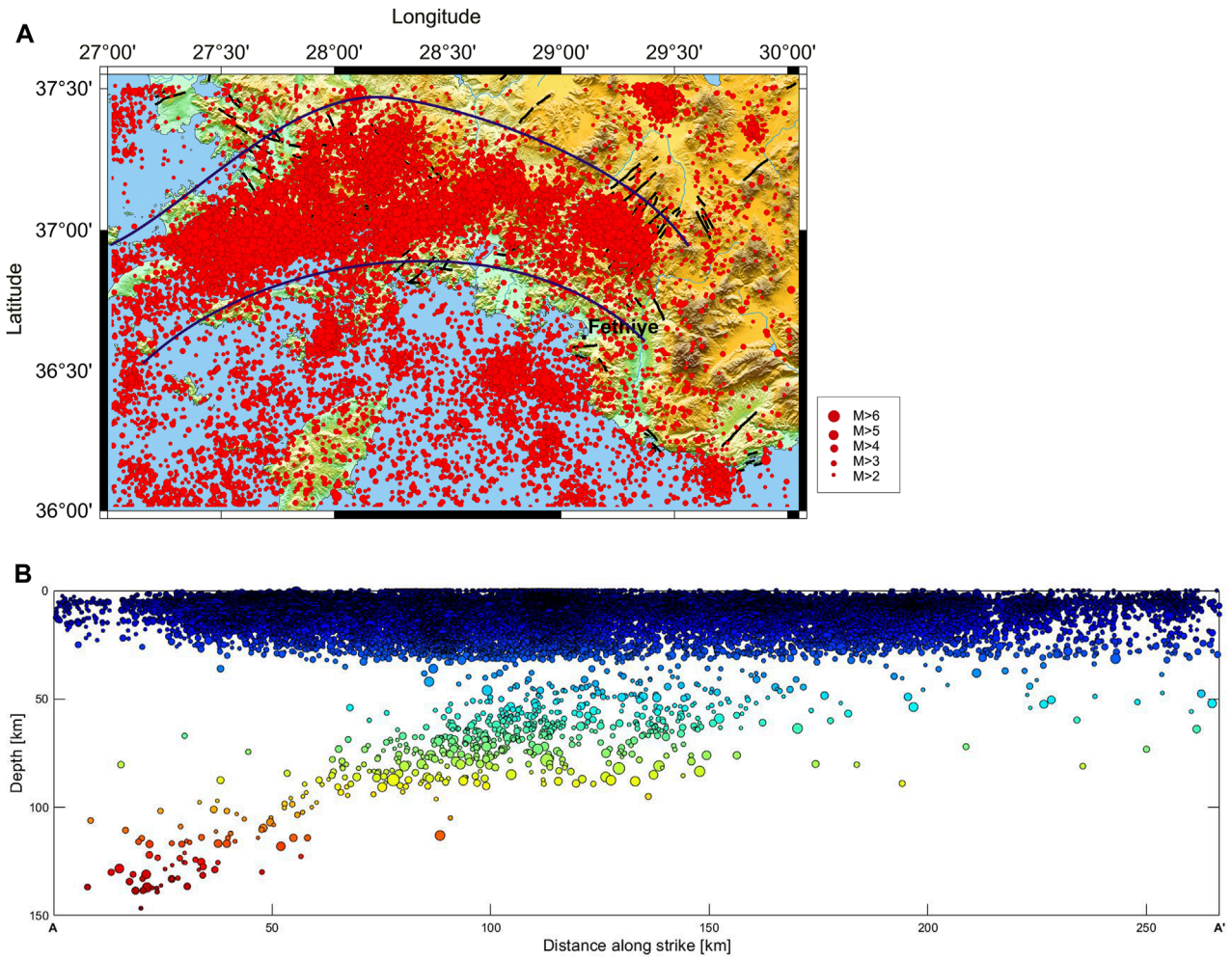

FIGURE 9
(A) Map of epicenters of earthquakes with Ml ≥ 2.0 between 2004 and 2020 occurred in the study region. Modified from Akar et al. (2022). **(B)** Map of epicenters of earthquakes with Ml ≥ 2.0 between 2004 and 2020 occurred in the study region. Modified from Akar et al. (2022).

According to (Elitez et al., 2016), GPS speeds and focal mechanisms of earthquakes show that there is no single transform fault along the Burdur-Fethiye region. According to (Koçyigit, 1984) the block faults active in Southwest Anatolia developed as normal faults intersecting each other in different directions. These fractures are faults with different directions but formed in the same period. As a matter of fact, in the magnetic anomaly map obtained by this study (Figure 3), elliptical magnetic anomalies representing these NESW, NW-SE, E-W, and N-S oriented faults are observed.

When the geological map, magnetic anomalies, and heat flow map are evaluated together, it is seen that the area where Jurassic Cretaceous ophiolites, known as the Lycian Nappes, are located, gives high magnetic anomalies. Heat flow values were also low in areas where earthquakes were intense. The deepest Curie values correlate well with large sedimentary units in the study area. It can be suggested from estimated zt values that the sediment thickness varies between 1.14 km and 4.17 km (Table 1).

4 Conclusion

In this study, the fractal-based centroid method in the wavenumber domain with the variable windows sizes (50–150 km) applied to the RTP anomalies of the magnetic data is used for the first time to determine the Curie point depths of the Cameli Basin and its surrounding area. The CPDs vary from about 6.9 to 14.05 km and the average CPD is 10.57 km in the study area. The CDP values are commonly associated with the type of basement (igneous and/or metamorphic) and volcanic rocks. It can be suggested from the CPD map that minimum circular contour closure in the east of Karamanli may include a high or medium geothermal potential area. The thermal gradient map of the study region shows that the thermal gradient varies from 41.28°C/km to 89.23°C/km and the average value is 58.59°C/km. The variation of earthquakes is generally concentrated in the south of Denizli and the west of Cameli. In the study area, the shallow Curie depths and moderate/small magnitude earthquakes are observed and may be associated with the active fault zones. In addition, the areas between lower and higher Curie

depths can be separated by the main faults in the study region. It is suggested that the depth of the magnetic basement can be located at the upper crust.

It is known that earthquakes occur at depths of more than 60 km in this region. If we associate this situation with the moho depth, the moho depth progresses much deeper in this region due to the effect of subduction. It can be said that the depth of the Curie isotherm is significantly shallower than the Moho depth. In this study, it was determined that the geothermal gradient was low in the regions where earthquakes were most intense. Considering the thermal structures obtained with aeromagnetic data, the earthquakes that have occurred, and the tectonism of the region, it is thought that the Curie depth (6.9–14.05 km) is not related to the depth to the deep asthenosphere and that mostly thermal structures are related to faults in the region or to the shallow asthenosphere depth where the continental crust is thin.

Data availability statement

The original contributions presented in the study are included in the article/supplementary material, further inquiries can be directed to the corresponding author.

Author contributions

FA: Conceptualization, Data curation, Formal Analysis, Investigation, Project administration, Resources, Validation, Visualization, Writing–original draft, Writing–review and editing.

Funding

The author(s) declare financial support was received for the research, authorship, and/or publication of this article. The aeromagnetic data included in the study were obtained from the General Directorate of Mineral Research and Research (MTA) in Türkiye within the scope of CUBAP Project: M567.

Conflict of interest

The author declares that the research was conducted in the absence of any commercial or financial relationships that could be construed as a potential conflict of interest.

Publisher's note

References

Abdullahi, M., and Kumar, R. (2020). Curie depth estimated from high-resolution aeromagnetic data of parts of lower and middle Benue trough (Nigeria). *Acta Geod. Geophys.* 55 (4), 627–643. doi:10.1007/s40328-020-00314-4

Akar, F., Akkoyunlu, M., and Bilim, F. (2022). The spatial analysis of b-values of the area between Bodrum and Fethiye districts, the south-western anatolia, Turkey. *Mühendislik Bilim. ve Tasar. Derg.* 10, 1, 238–246. doi:10.21923/jesd.982238

Akar, F., and Bilim, F. (2022). Determination of crustal structure beneath the Cameli Basin (SW Turkey) using an aeromagnetic data. *Electron. Lett. Sci. Eng.* 18 2, 31–40.

Alcicek, M. C., Kazanci, N., and Ozkul, M. (2005). Multiple rifting pulses and sedimentation pattern in the Çameli Basin, southwestern Anatolia, Turkey. *Sediment. Geol.* 173, 409–431. doi:10.1016/j.sedgeo.2003.12.012

Alcicek, M. C., Ten Veen, J. H., and Ozkul, M. (2006). "Neotectonic development of the Cameli Basin, southwestern anatolia, Turkey," in *Tectonic development of the eastern mediterranean region*. Editors A. H. F. Robertson, and D. Mountrakis (Geological Society London), 260, 591–611. doi:10.1144/GSL.SP.2006.260.01.25

Alptekin, Ö. (1973). *Focal mechanisms of earthquakes in western Turkey and their tectonic implications*. United States: PhD thesis, New Mexico Institute of Mining and Technology. Diss.

Ates, A., Bilim, F., and Buyuksarac, A. (2005). Curie point depth investigation of Central Anatolia, Turkey. *Pure Appl. Geophys.* 162, 357–371. doi:10.1007/s00024-004-2605-3

Ates, A., Bilim, F., Buyuksarac, A., Aydemir, A., Bektas, O., and Aslan, Y. (2012). Crustal structure of Turkey from aeromagnetic, gravity and deep seismic reflection data. *Surv. Geophys.* 33, 869–885. doi:10.1007/s10712-012-9195-x

Ates, A., Kearey, P., and Tufan, S. (1999). New gravity and magnetic anomaly maps of Turkey: new gravity and magnetic anomaly maps of Turkey. *Geophys. J. Int.* 136, 499–502. doi:10.1046/j.1365-246X.1999.00732.x

Ates, A., Sevinc, A., Kadioglu, Y. K., and Kearey, P. (1997). Geophysical investigation of the deep structure of the Aydin-Milas region. Southwest Turkey, Evidence from the possible extension of the Hellenic Arc. *Israel J. Earth Sci.* 46, 29–40.

Aydemir, A., Bilim, F., Kosaroglu, S., and Buyuksarac, A. (2019). Thermal structure of the Cappadocia region, Turkey, a review with geophysical methods. *Mediterr. Geosci. Rev.* 1, 243–254. doi:10.1007/s42990-019-00011-7

Aydin, I., Karat, H. I., and Kocak, A. (2005). Curie-point depth map of Turkey. *Geophys. J. Int.* 162, 633–640. doi:10.1111/j.1365-246X.2005.02617.x

Baldwin, R. T., and Langel, R. (1993). Tables and maps of the DGRF 1985 and IGRF 1990. *IAGA Bull.* 54, 158.

Berry, M. V., Lewis, Z. V., and Nye, J. F. (1980). On the Weierstrass-Mandelbrot fractal function. *Proc. R. Soc. Lond. A Math. Phys. Sci.* 370 (1743), 459–484. doi:10.1098/rspa.1980.0044

Bhattacharyya, B. K., and Leu, L. (1975). Analysis of magnetic anomalies over Yellowstone National Park, mapping of Curie point isothermal surface for geothermal reconnaissance. *J. Geophys Res.* 80, 4461–4465. doi:10.1029/JB080i032p04461

Bilim, F. (2007). Investigations into the tectonic lineaments and thermal structure of Kutahya–Denizli region, western Anatolia, from using aeromagnetic, gravity and seismological data. *Phys. Earth Planet. Interiors* 165 (3-4), 135–146. doi:10.1016/j.pepi.2007.08.007

Bilim, F., Akay, T., Aydemir, A., and Kosaroglu, S. (2016). Curie point depth, heat flow and radiogenic heat production deduced from the spectral analysis of the aeromagnetic data for geothermal investigation on the Menderes massif and the Aegean region, western Turkey. *Geothermics* 60, 44–57. doi:10.1016/j.geothermics.2015.12.002

Blakely Richard, J. (1996). *Potential theory in gravity and magnetic applications*. Cambridge: Cambridge University Press.

Bozkurt, E. (2001). Neotectonics of Turkey–a synthesis. *Geodin. acta* 14, 3–30. doi:10.1016/s0985-3111(01)01066-x

Bozkurt, E. (2004). Granitoid rocks of the southern Menderes Massif (southwestern Turkey): field evidence for Tertiary magmatism in an extensional shear zone. *Int. J. Earth Sci.* 93, 52–71. doi:10.1007/s00531-003-0369-0

Bozkurt, E., and Oberhansli, R. (2001). Menderes massif. (western Turkey), structural, metamorphic and magmatic evolution-a synthesis. *Int. J. Earth Sci.* 89, 679–708. doi:10.1007/s005310000173

Bozkurt, E., and Park, R. G. (1994). Southern Menderes Massif, an incipient metamorphic core complex in western Anatolia, Turkey. *J. Geol. Soc. Lond.* 151, 213–216. doi:10.1144/gsjgs.151.2.0213

Bozkurt, E., and Sozbilir, H. (2001). Tectonic evolution of the Gediz graben, field evidence for an episodic, two-stage extension in western Turkey. *Geol. Mag.* 141, 63–79. doi:10.1017/S0016756803008379

Büyüksaraç, A. (2005). Tectonomagmatic evolution of bimodal plutons in the central Anatolian crystalline complex, Turkey: a discussion. *J. Geol.* 113 4, 495–496. doi:10.1086/430245

Connard, G., Couc, R., and Gemperle, M. (1983). Analysis of aeromagnetic measurements from the Cascade Range in central Oregon. *Geophysics* 48, 376–390. doi:10.1190/1.1441476

Çubuk, Y. (2010). *2005-2008 bâla-sıraplnar (ankara) ve Cameli (denizli) depremlerinin kaynak mekanizması parametreleri*. Turkey: PhD Thesis. İstanbul Teknik Üniversitesi, Fen Bilimleri Enstitüsü.

Demirtaş, R. (2018). Helenik-kıbrıs yay sistemi diri fayları, paleosismolojik çalışmalar ve gelecek deprem potansiyelleri. Available at: https://www.academia.edu/88274457/HELEN%C4%B0K_KIBRIS_YAY_S%C4%B0STEM%C4%B0_D%C4%B0R%C4%B0_FAYLARI_PALEOS%C4%B0SMOLOJ%C4%B0K_%C3%87ALI%C5%9EMALAR_VE_GELECEK_DEPREM_POTANS%C4%B0YELER%C4%B0, Accessed: 10 July 2021. doi:10.13140/RG.2.2.35140.68487

Dewey, J. F., and Sengör, A. M. C. (1979). Aegean and surrounding regions: complex multiplate and continuum tectonics in a convergent zone. *Geol. Soc. Am. Bull.* 90 1, 84–92. doi:10.1130/0016-7606(1979)90<84:AASRCM>2.0.CO;2

Dilek, Y., and Altunkaynak, S. (2007). Cenozoic crustal evolution and mantle dynamics of post-collisional magmatism in western anatolia. *Int. Geol. Rev.* 49, 431–453. doi:10.2747/0020-6814.49.5.431

Dolmaz, M. N. (2007). An aspect of the subsurface structure of the Burdur-Isparta area, SW Anatolia, based on gravity and aeromagnetic data, and some tectonic implications. *Earth Planets Space* 59, 5–12. doi:10.1186/BF03352016

Dolmaz, M. N., Hisarli, Z. M., Ustaomer, T., and Orbay, N. (2005). Curie point depths based on spectrum analysis of aeromagnetic data, West Anatolian extensional province, Turkey. *Pure Appl. Geophys.* 162, 571–590. doi:10.1007/s00024-004-2622-2

Elitez, I., and Yaltirak, C. (2016). Miocene to Quaternary tectonostratigraphic evolution of the middle section of the Burdur-Fethiye Shear Zone, south-western Turkey: implications for the wide inter-plate shear zones. *Tectonophysics* 690, 336–354. doi:10.1016/j.tecto.2016.10.003

Elitez, I., Yaltırak, C., and Aktug, B. (2016). Extensional and compressional regime driven left-lateral shear in southwestern Anatolia. (eastern Mediterranean), the Burdur– Fethiye Shear Zone. *Tectonophysics* 688, 26–35. doi:10.1016/j.tecto.2016.09.024

Elitok, Ö., and Dolmaz, M. N. (2008). Mantle flow-induced crustal thinning in the area between the easternmost part of the Anatolian plate and the Arabian Foreland (E Turkey) deduced from the geological and geophysical data. *Gondwana Res.* 13 (3), 302–318. doi:10.1016/j.gr.2007.08.007

Erbek, E., and Dolmaz, M. N. (2019). Investigation of the thermal structure and radiogenic heat production through aeromagnetic data for the southeastern Aegean Sea and western part of Turkey. *Geothermics* 81, 113–122. doi:10.1016/j.geothermics.2019.04.011

Ergin, K. (1966). Türkiye ve civarının episantr haritası hakkında. *Türkiye Jeol. Bülteni* 10 1-2, 122–129.

Fedi, M., Quarta, T., and De Santis, A. (1997). Inherent power-law behavior of magnetic field power spectra from a Spector and Grant ensemble. *Geophysics* 61, 1143–1150. doi:10.1190/1.1444215

Gokten, E., Havzaoglu, T., and San, O. (2001). Tertiary evolution of the central Menderes Massif based on structural investigations of metamorphics and sedimentary cover rocks between Salihli and Kiraz (western Turkey). *Int. J. Earth Sci.* 89, 745–756. doi:10.1007/s005310000099

Haklidir, F. S. T., and Haklidir, M. (2020). Prediction of reservoir temperatures using hydrogeochemical data, western Anatolia geothermal systems (Turkey), a machine learning approach. *Nat. Resour. Res.* 29, 2333–2346. doi:10.1007/s11053-019-09596-0

Hetzel, R., Passchier, C. W., Ring, U., and Dora, O. O. (1995). Bivergent extension in orogenic belts, the Menderes Massif (southwestern Turkey). *Geology* 23, 455–458. doi:10.1130/0091-7613(1995)023<0455,BEIOBT>2.3.CO;2

Ilkisik, O. M. (1995). Regional heat flow in western Anatolia using silica temperature estimates from thermal springs. *Tectonophysics* 244, 175–184. doi:10.1016/0040-1951(94)00226-Y

Khojamli, A., Doulati Ardejani, F., Moradzadeh, A., Nejati Kalateh, A., Roshandel Kahoo, A., and Porkhial, S. (2017). Determining fractal parameter and depth of magnetic sources for Ardabil geothermal area using aeromagnetic data by de-fractal approach. *J. Min. Environ.* 8 (1), 93–101. doi:10.22044/jme.2015.481

Koçyigit, A. (1984). *Tectono-stratigraphic characteristics of hoyran lake region (isparta bend). Geology of the taurus belt*. Turkey, Ankara: MTA, Geol. soc.

Li, C. F., Chen, B., and Zhou, Z. Y. (2009). Deep crustal structures of eastern China and adjacent seas revealed by magnetic data. *Sci. China Ser. D, Earth Sci.* 52, 984–993. doi:10.1007/s11430-009-0096-x

Li, C. F., Zhou, D., and Wang, J. (2019). On application of fractal magnetization in Curie depth estimation from magnetic anomalies. *Acta Geophys.* 67, 1319–1327. doi:10.1007/s11600-019-00339-6

Lowell, R. P., and Rona, P. A. (2005). Tektonics/hydrothermal activity. *Encycl. Geol.*, 362–372.

Ma, M., Xiu, L., Gao, Q., Li, Y., Wang, W., Xu, H., et al. (2023). An aeromagnetic denoising-decomposition-3D inversion approach for mineral exploration. *Front. Earth Sci.* 11, 1132093. doi:10.3389/feart.2023.1132093

Nabi, S. H. A. E. (2012). Curie point depth beneath the Barramiya–Red Sea coast area estimated from spectral analysis of aeromagnetic data. *J. Asian Earth Sci.* 43, 254–266. doi:10.1016/j.jseaes.2011.09.015

Okubo, Y., Graf, R. J., Hansen, R. O., Ogawa, K., and Tsu, H. (1985). Curie point depths of the Island of Kyushu and surrounding areas, Japan. *Jpn. Geophys.* 50, 481–494. doi:10.1190/1.1441926

Oner, Z., and Dilek, Y. (2013). Fault kinematics in supra detachment basin formation, Menderes core complex of western Turkey. *Tectonophysics* 608, 1394–1412. doi:10.1016/j.tecto.2013.06.003

Över, S., Demirci, A., and Özden, S. (2023). Tectonic implications of the february 2023 earthquakes (Mw7. 7, 7.6 and 6.3) in south-eastern Türkiye. *Tectonophysics* 866, 230058. doi:10.1016/j.tecto.2023.230058

Over, S., Ozden, S., Pınar, A., Yılmaz, H., Unlugenc, U. C., and Kamacı, Z. (2010). Late cenozoic stress field in the Cameli Basin, SW Turkey. *Tectonophysics* 492, 60–72. doi:10.1016/j.tecto.2010.04.037

Özkaptan, M., Kaymakci, N., Langereis, C. G., Gülyüz, E., Özacar, A. A., Uzel, B., et al. (2018). Age and kinematics of the Burdur basin: inferences for the existence of the Fethiye Burdur Fault Zone in SW anatolia (Turkey). *Tectonophysics* 744, 256–274. doi:10.1016/j.tecto.2018.07.009

Pamukçu, O., Akçığ, Z., Hisarlı, M., and Tosun, S. (2014). Curie Point depths and heat flow of eastern Anatolia (Turkey). *Energy Sources, Part A Recovery, Util. Environ. Eff.* 36 (24), 2699–2706. doi:10.1080/15567036.2011.574194

Pamukcu, O., Gonenc, T., Cırmık, A., Pamukcu, C., and Erturk, N. (2019). The geothermal potential of Buyuk Menderes Graben obtained by combined 2.5 D normalized full gradient results. *Pure Appl. Geophys.* 176, 5003–5026. doi:10.1007/s00024-019-02227-y

Pilkington, M., and Todoeschuck, J. P. (1993a). Fractal magnetization of continental crust. *Geophys. Res. Lett.* 20 (7), 627–630. doi:10.1029/92GL03009

Pilkington, M., and Todoeschuck, J. P. (1993b). Fractal magnetization of continental crust. *Geophys. Res. Lett.* 20 (7), 627–630. doi:10.1029/92GL03009

Reilinger, R., McClusky, S., Paradissis, D., Ergintav, S., and Vernant, P. (2010). Geodetic constraints on the tectonic evolution of the Aegean region and strain accumulation along the Hellenic subduction zone. *Tectonophysics* 488, 22–30. doi:10.1016/j.tecto.2009.05.027

Roche, V., Bouchot, V., Beccaletto, L., Jolivet, L., Goillou-Frottier, L., Tuduri, J., et al. (2018). Structural, lithological, and geodynamic controls on geothermal activity in the Menderes geothermal Province. (western Anatolia, Turkey). *Int. J. Earth Sci.* 108, 301–328. doi:10.1007/s00531-018-1655-1

Ross, H. E., Blakely, R. J., and Zoback, M. D. (2006). Testing the use of aeromagnetic data for the determination of Curie depth in California. *Geophysics* 71, 51–59. doi:10.1190/1.2335572

Saunders, P., Priestley, K., and Taymaz, T. (1998). Variations in the crustal structure beneath western Turkey. *Geophys. J. Int.* 134, 373–389. doi:10.1046/j.1365-246x.1998.00571.x

Schmid, S. M., Fugenschuh, B., Kounov, A., Matenco, L., Nievergelt, P., Oberhansli, R., et al. (2020). Tectonic units of the Alpine collision zone between Eastern Alps and western Turkey. *Gondwana Res.* 78, 308–374. doi:10.1016/j.gr.2019.07.005

Sengor, A. M. C., Satır, M., and Akkok, R. (1984). Timing of tectonic events in the Menderes Massif, western Turkey, implications for tectonic evolution and evidence for Pan-African basement in Turkey. *Tectonics* 3, 693–707. doi:10.1029/TC003i007p00693

Sengor, A. M. C., and Yilmaz, Y. (1981). Tethyan evolution of Turkey, A plate tectonic approach. *Tectonophysics* 75, 181–241. doi:10.1016/0040-1951(81)90275-4

Seyitoglu, G., Isık, V., and Cemen, İ. (2004). Complete Tertiary exhumation history of the Menderes massif, western Turkey, an alternative working hypothesis. *Terra nova.* 16, 358–364. doi:10.1111/j.1365-3121.2004.00574.x

Shirani, S., Nejati Kalateh, A., and Noorollahi, Y. (2020). Curie point depth estimations for northwest Iran through spectral analysis of aeromagnetic data for geothermal resources exploration. *Nat. Resour. Res.* 29, 2307–2332. doi:10.1007/s11053-019-09579-1

Spector, A., and Grant, F. S. (1970). Statistical models for interpretation aeromagnetic data. *Geophysics* 35, 293–302. doi:10.1190/1.1440092

Teen Veen, J. H., Boulton, S. J., and Alcicek, M. C. (2009). From palaeotectonics to neotectonics in the Neotethys realm, the importance of kinematic decoupling and inherited structural grain in SW Anatolia. (Turkey). *Tectonophysics* 473, 261–281. doi:10.1016/j.tecto.2008.09.030

Turcotte, D. L., and Schubert, G. (1982). *Applications of continuum physics to geological problems*. John Wiley and Sons.

Westaway, R. (2006). Cenozoic cooling histories in the Menderes Massif, western Turkey, may be caused by erosion and flat subduction, not low-angle normal faulting. *Tectonophysics* 412, 1–25. doi:10.1016/j.tecto.2005.08.005

Yaltırak, C., Elitez, İ., Aksu, A., Hall, J., Çifçi, G., Remzi, D. D., et al. (2010). The relationship and evolution of the burdur-fethiye Fault Zone, the rhode basin, anaximender seamounts, the antalya Gulf, and the isparta angle since Miocene to recent in tectonics of the eastern mediterranean.

Yaro, U. Y., Abir, I. A., and Balarabe, B. (2023). Determination of Curie point depth, heat flow, and geothermal gradient to infer the regional thermal structure beneath the Malay Peninsula using de-fractal method. *Arabian J. Geosciences* 16 (1), 84. doi:10.1007/s12517-022-11164-5